Calculation of Fe–B–V ternary phase diagram

Viera Homolová [a,*], Aleš Kroupa [b], Anna Výrostková [a]

[a] Institute of Materials Research, Slovak Academy of Sciences, Watsonova 47, Košice 040 01 Slovakia
[b] Institute of Physics of Materials, Academy of Sciences of Czech Republic, Žižkova 22, Brno, Czech Republic

ARTICLE INFO

ABSTRACT

The phase equilibria of the Fe–B–V ternary system are studied experimentally and theoretically in this paper. Phase diagram of the system was modelled by CALPHAD method. Boron was modelled as an interstitial element in the FCC and BCC solid solutions. The calculations of isothermal sections of phase diagram are compared with our experimental results at 903 and 1353 K and with available literature experimental data. New ternary phase (with chemical composition 28Fe32V40B in at.%) was found in 67Fe–18B–15V alloy [in at.%]. Further experimental studies for the determination of exact nature of the ternary phase including crystallographic information are necessary.

© 2011 Elsevier B.V. All rights reserved.

1. Introduction

The knowledge about phase equilibria of the Fe–B–V system is important in several fields of materials research. The elements as vanadium and boron are added into various complex alloys, e.g. modified ferritic and austenitic steels for energy industry. Boron is used to increase their hardenability [1], and vanadium is strong boride-forming element forming stabile borides with high melting temperatures, hardness and wear resistance.

Generally, the ternary Fe–B–V system was not studied experimentally very intensively. Only the work of Kuzma and Starodub [2] is known from literature. They studied experimentally phase equilibria of the system at 1073 K after 300 h of annealing by X-ray diffraction on a series of alloys covering most of the phase diagram. Since then no new experimental or theoretical information about the system has been published.

The present work is focused on the modelling of the Fe–B–V system by Calphad method using our experimental results besides those found in literature.

2. Experimental procedure

Model alloys were prepared in argon arc furnace from elements of high purity: Fe (99.98%), V (99.8%) and B (99.9%). Chemical composition of the alloys is given in Table 1. The batches (10–20 g) were re-melted several times to achieve proper homogeneity. This process was connected with weight loss of 0.5–1 g in the case of

20 g batches. Samples evacuated and sealed in silica glass ampoules were annealed at 1353 K and 903 K for various times up to 60 days (for 1353 K) and 190 days (for 903 K). The ampoules were broken and samples quenched immediately in water after annealing.

The experimental material was studied by means of the electron microprobe analysis and scanning electron microscopy (EDXS, JEOL JSM-7000F "Thermal FEG"). This analyser enables quantitative element analysis for elements from atomic number 5 (boron). The structure of alloys was studied by X-ray diffraction (Philips X'Pert Pro) and selected samples also by Electron Back Scattered Diffraction (EBSD) method.

3. Thermodynamic model

The thermodynamic sublattice model developed by Hillert and Staffansson [3] was used in the present work to describe the Gibbs energies of individual phases.

Boron was considered as an interstitial element or a substitutional element in solid solution of iron (BCC, FCC) in the past by various authors [4–6]. It is rather difficult to decide whether boron atoms behave interstitially or substitutionally because of very low solubility of B in iron. Van Rompacy et al. [4] modelled boron both as an interstitial and a substitutional element in BCC phase in their theoretical assessment of the Fe–B system and created two equivalent datasets for the modelling of this system. Both descriptions (B as an interstitial element or a substitutional one) are needed when the binary system is extrapolated to high-order systems. For example B is modelled as an interstitial element in Fe–B–Ti system [5], and as a substitutional element in Fe–B–Nd system [6]. According to Guo and Kelly [7] elements as Cr, Mo and V increase solubility of boron in iron solution, because their atom diameters are lager than

Table 1
Chemical compositions of alloys and conditions of annealing.

Alloy	Composition [at.%]	Annealing
1	52Fe–10B–38V	1353 K/70 days
2	67Fe–18B–15V	1353 K/60 days
3	68Fe–27B–5V	1353 K/60 days
4	13Fe–25B–62V	903 K/190 days
		1353 K/60 days
5	32Fe–13B–55V	1353 K/30 days
6	50Fe–41B–9V	1353 K/60 days
		903 K/190 days
7	30Fe–60B–10V	903 K/190 days
8	19Fe–51B–30V	903 K/190 days
9	30Fe–38B–32V	1353 K/60 days
10	22Fe–44B–34V	903 K/190 days

that of iron and they form substitutional solid solution with iron, resulting in the expansion of the size of interstitial position. That is why boron is considered as interstitial element in BCC and FCC solid solutions for the investigated Fe–B–V system in this paper.

3.1. Thermodynamic models for solid solution phases (BCC and FCC) and liquid

Gibbs energies for BCC and FCC phases in the Fe–B–V system were described using the two-sublattice model containing metal and interstitial elements, respectively. Iron and vanadium can substitute for each other in the metal sublattice, similarly as B and vacancies in the interstitial sublattice. For one formula unit $(Fe,V)_a(B,Va)_c$, the model gives

$$G_m = \sum_i y_i(y_B + G^o_{i:B} + y_{Va}G^o_{i:Va}) + aRT\sum_i y_i \ln y_i + cRT(y_B \ln y_B$$

$$+ y_{Va} \ln y_{Va}) + y_{Fe}y_V(y_B L_{Fe,V:B} + y_{Va}L_{Fe,V:Va}) + y_B y_{Va}\sum_i y_i L_{i:B,Va}$$

$$+ + G_{mag} \quad i = Fe, \quad V. \tag{1}$$

In Eq. (1), y denotes the site fraction of component i in the relevant sublattice. Symbols a and c denote the numbers of sites in each sublattice. In the case of BCC: $a = 1$ and $c = 3$, for FCC: $a = c = 1$. Components in different sublattices are separated by colon and in the same sublattice by comma. $G^o_{i:Va}$ is the Gibbs energy of pure element i in a structure corresponding to BCC or FCC phase and relevant non-magnetic state and $G^o_{i:B}$ is the Gibbs energy of a hypothetical non-magnetic state, where all interstitial sites in the BCC or FCC structure are occupied by boron. All values of G are given relative to the reference state that is defined as a standard state at 298.15 K and 10^5 Pa. The excess Gibbs energy is defined by the temperature and concentration dependent interaction parameter L. The concentration dependence is expressed by Redlich–Kister polynomial (Eq. (2)) as

$$L_{i,j:k} = \sum_{v=0}^n L^v_{i,j:k}(y_i - y_j)^v \quad i, j = Fe, V \quad k = B, Va \tag{2}$$

The temperature dependence of the parameter L^v is expressed by Eq. (3)

$$L^v_{i,j:k} = A + BT \tag{3}$$

G_{mag} is the magnetic part of the Gibbs energy.

Liquid is described using a model with one sublattice where metallic components and B are mixed together. Gibbs energy of

liquid phase is described by the following equation

$$G_m = \sum_i y_i G^0_i + RT\sum_i y_i \ln y_i + \sum_i \sum_j y_i y_j L_{i,j}$$

$$+ \sum_i \sum_j \sum_k y_i y_j y_k L_{i,j,k} \quad i, j, k = Fe, V, B \quad but \quad i \ne j \ne k. \tag{4}$$

3.2. Thermodynamic model for sigma phase

Sigma phase is described with three-sublattice model with formula $(Fe)_8(V)_4(Fe,V,B)_{18}$. Its Gibbs energy is given as follows:

$$G_m = \sum_i y^I_{Fe}y^{II}_V y^{III}_i G^o_{Fe:V:i} + 8RTy^I_{Fe}\ln y^I_{Fe} + 4RTy^{II}_V \ln y^{II}_V$$

$$+ 18RT\sum_i y^{III}_i \ln y^{III}_i + \sum_i \sum_j y^I_{Fe}y^{II}_V y^{III}_i y^{III}_j L_{Fe:V:i,j}$$

$$+ y^I_{Fe}y^{II}_V y^{III}_{Fe}y^{III}_V y^{III}_B L_{Fe:V:Fe,V,B} \quad i, j = Fe, V, B \quad with \quad i \ne j. \tag{5}$$

Numbers I, II and III denote the sublattice.

3.3. Thermodynamic model for borides (FeB, Fe₂B, V₃B₂, VB, V₅B₆, V₃B₄, V₂B₃, VB₂, T-ternary phase) and β-rhombohedral B

The borides are described as stoichiometric phases (with respect to the amount of boron) with the two-sublattice model where iron and vanadium mix themselves in one sublattice and the other sublattice is filled with boron. For one formula unit $(Fe,V)_a(B)_c$ of a boride, the model gives

$$G_m = \sum_i y_i y_B G^0_{i:B} + aRT\sum_i y_i \ln y_i + cRTy_B \ln y_B$$

$$+ y_{Fe}y_V y_B L_{Fe,V:B} \quad i = Fe, V. \tag{6}$$

The ternary phase that was found within the scope of this work was described as a stoichiometric phase with three-sublattice model with formula $(V)_{0.32}(Fe)_{0.28}(B)_{0.4}$.

The β-rhombohedral B phase is modelled as stoichiometric phase.

The calculations of phase equilibria were performed by Thermo-Calc software [8]. The thermodynamic parameters for binary Fe–V and Fe–B systems were taken from the literature [4,9] and the data for pure elements were taken from Dinsdale [10]. The thermodynamic description of V–B system, including the parameters for vanadium borides, was taken from SSOL database [11] except for V₅B₆ boride that is missing in this database. The parameters of the V₅B₆ were assessed in the scope of this work. The SSOL database [11] defined boron as substitutional element in the BCC phase for V–B system. That is why the BCC phase with the boron as interstitial element was reassessed in the scope of this work. The phase diagrams of Fe–V and V–B binary subsystems are shown in Fig. 1

Binary data can be used for ternary extrapolation from the constituent binary systems. The prediction offers basic information on phase equilibria in the system but does not offer information on any ternary phase or solubility of third element in binary phases. The ternary interaction parameters for the phases, which described the solubility of the third element, were determined on the basis of our experimental results and work [2]. The experimental results were used also for determination of parameters for new ternary phase T.
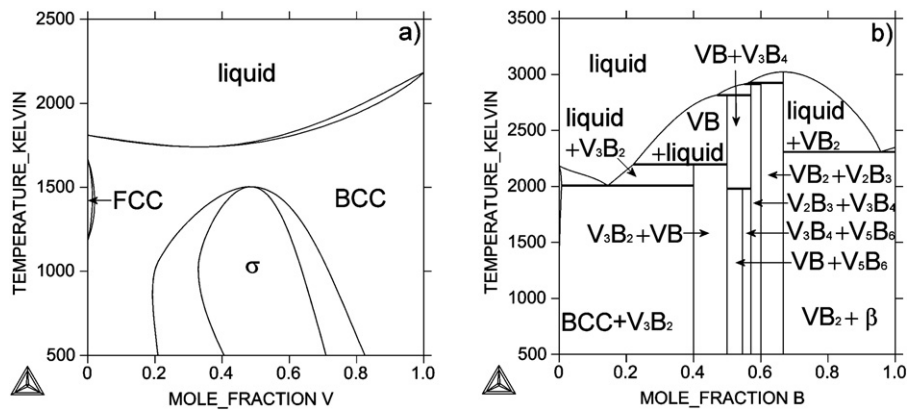
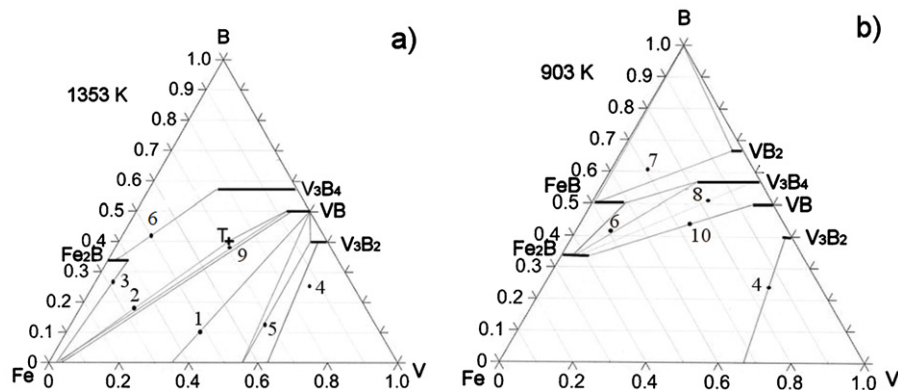**Fig. 1.** Phase diagrams of the binary subsystems (a) Fe–V and (b) V–B.

Fig. 2. Isothermal section of phase diagram constructed with using experimental results. Model alloys are marked by black points. At (a) 1353 K and (b) 903 K.

4. Experimental results

Isothermal sections of the phase diagram at 1353 K and 903 K were constructed using the results of alloy phase analyses, Fig. 2. The nominal composition of alloys is marked in the figure. With respect to the number of alloys, the constructed diagram does not cover complete phase diagram of the ternary system. Examples of the microstructures of investigated alloys are presented in Figs. 3 and 4. Experimentally determined phase compositions at given temperatures are shown in Table 2. The phase identification was carried out by X-ray diffraction and for selected samples also by EBSD. An unknown ternary phase was found in alloy 2 (67Fe–18B–15V in at.%) at 1353 K with chemical composition approx. 28 at.% Fe, 32 at.% V and 40 at.% B. It is marked by T in Fig. 3.

All borides exhibit solubility of third element. It was found that Fe_2B contains up to 7 at.% of vanadium and FeB dissolves up to 9 at.%

Table 2
Phases identified in the model alloys after annealing.

Alloy	Identified phases	
	1353 K	903 K
1	BCC, VB	
2	BCC, VB, T	
3	Fe_2B, BCC	
4	V_3B_2, BCC	BCC, VB, V_3B_2
5	VB, V_3B_2, sigma	
6	Fe_2B, V_3B_4	FeB, Fe_2B, V_3B_4
7		FeB, VB_2, β
8		V_3B_4, Fe_2B
9	BCC, VB	
10		VB, Fe_2B

of V. Similarly various amounts of dissolved iron were measured in vanadium borides. In particular, VB dissolves up to 7 at.% of Fe, V_3B_2 contains up to 4 at.% of Fe, V_3B_4 dissolves up to 22 at.% of Fe and VB_2 contains up to 3 at.% of Fe.

5. Theoretical results and discussion

The database developed in the scope of this work, Table 3, was used for the calculation of phase diagram of the Fe–B–V system. Boron was modelled as interstitial element in BCC and FCC phase, all borides and the new ternary phase were modelled as stoichiometric phases.

The results of experimental part of the work were used for verification of the phase diagram. The achievement of the phase equilibrium in the alloys is very important for this comparison. The phase analysis and composition analysis of identified phases in as-cast alloys and after annealing for various times were compared. The analysis showed changes in phase composition and chemical composition of phases in annealed samples compared to the as-cast samples. However the changes are very small after 60 days compared to the samples annealed for 30 days. For example: in 2 alloy ratio of elements Fe:V in BCC phase has been 96:4 in as cast state, after annealing for 30 days the ratio was changed to 98:2, and for 60 days it was same as for 30. Therefore the model alloys can be considered as close enough to equilibrium after 60-day exposition at 1353 K and 190-day exposition at 903 K.
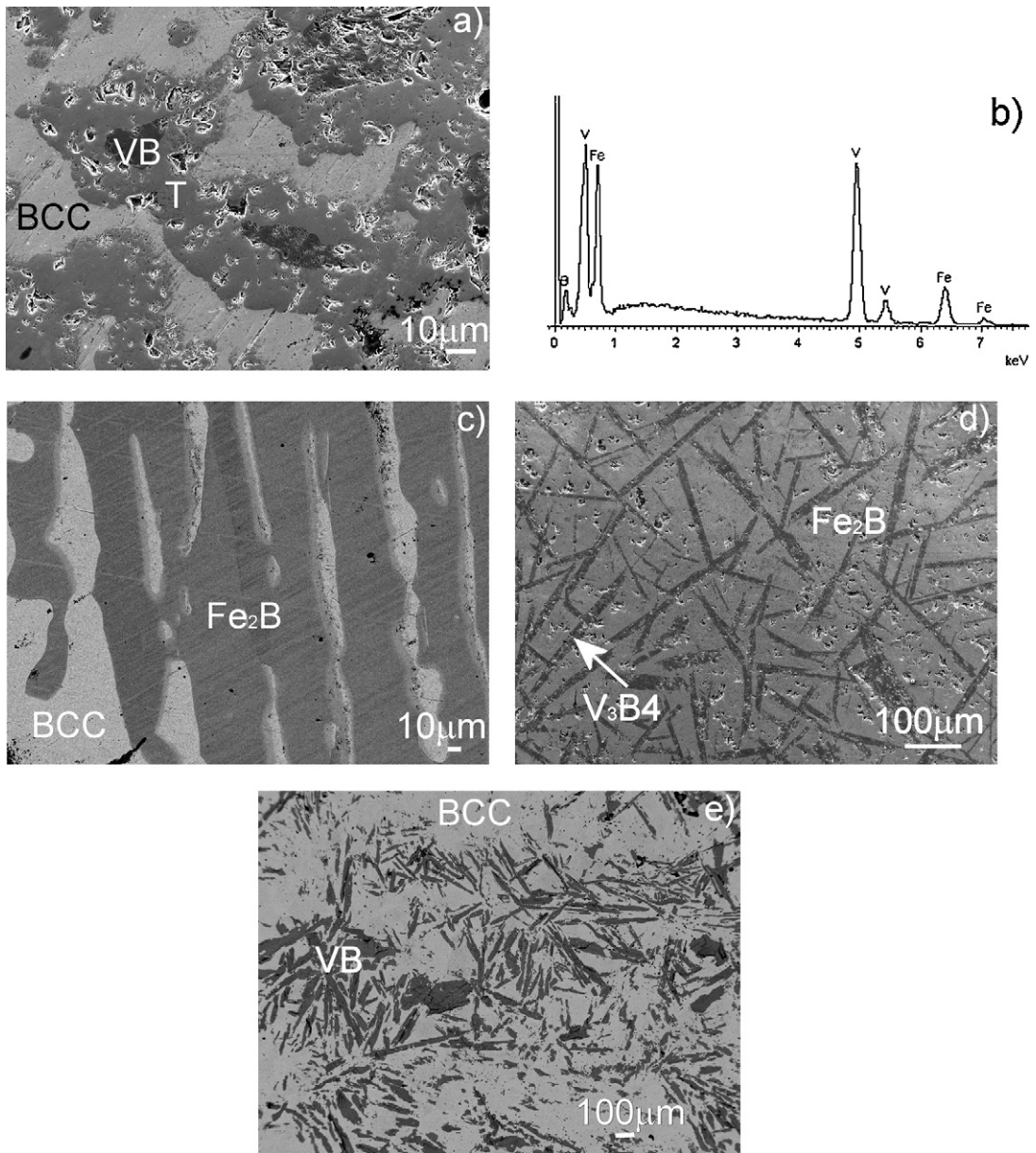
5.1. Comparison of calculations with experimental results

Three isothermal sections at 1353, 1073 and 903 K were mod-elled, see Fig. 5. The sections at 1353 K and at 903 K were compared
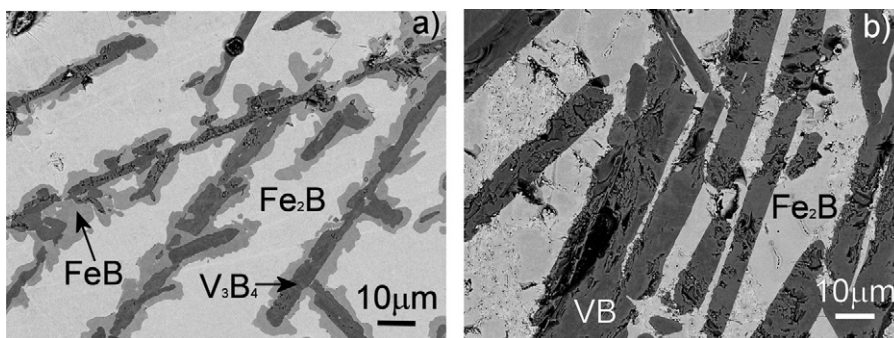
Fig. 3. Microstructure of Fe–B–V alloys after annealing at 1353 K for 60 days. (a) Alloy 2, (b) EDX spectrum of T-phase in alloy 2, (c) alloy 3, (d) alloy 6, and (e) alloy 9.

Fig. 4. Microstructure of Fe–B–V alloys after annealing at 903 K for 190 days. (a) Alloy 6 and (b) alloy 10.

Table 3
Thermodynamic parameters for ternary Fe–B–V system.

LIQUID
constituents: B, Fe, V
$^L L_{B,V;0} = -210,000 + 40^*T$ 298.00 < T < 4000.00
$^L L_{B,V;1} = -20,000$ 298.00 < T < 4000.00
$^L L_{B,V;2} = 40,000$ 298.00 < T < 4000.00
BCC_A2
2 sublattices, sites 1:3
constituents: Fe,V:B,Va
$^{BCC}G_{V:B;0} - 3^*H298(BETA\_rhombo\_b,B;0) - H298(BCC\_A2,V;0) = GVBCC$
$+ 3^*GBBETA - 170,000 + 67^*T$
no ternary parameters
BETA_RHOMBO_B
constituents: B
no ternary parameters
FCC_A1
2 sublattices, sites 1:1
constituents: Fe,V:B,Va
$^{FCC}G_{V:B;0} - H298(BETA\_rhombo\_b,B;0) - H298(BCC\_A2,V;0) = GVBCC + GBBETA$
no ternary parameters
Fe₂B
2 sublattices, sites 2:1
constituents: Fe,V:B
$^{Fe_2B}G_{V:B;0} - H298(BETA\_rhombo\_b, B; 0) - 2.0^*H298(BCC\_A2, V; 0) =$
$2^*GVBCC + GBBETA + 15,000$
$^{Fe_2B}L_{Fe,V:B;0} = -254,623.38 + 54.462^*T$ 298.00 < T < 4000.00
FeB
2 sublattices, sites 1:1
constituents: Fe,V:B
$^{FeB}G_{V:B;0} - H298(BETA\_rhombo\_b,B;0) - H298(BCC\_A2,V;0) = GVBCC + GBBETA$
$+ 15,000$
$^{FeB}L_{Fe,V:B;0} = -234,140.0 + 46.667^*T$ 298.00 < T < 4000.00
$^{FeB}L_{Fe,V:B;1} = 31,000$ 298.00 < T < 4000.00
SIGMA
3 sublattices, sites 8:4:18
constituents: Fe:V:B,Fe,V
$^{SIGMA}G_{Fe:V:B;0} - 18^*H298(BETA\_rhombo\_b,B;0) - 8^*H298(FCC\_A1,FE;0)$
$- 4^*H298(BCC\_A2,V;0) = 4^*GVBCC + 8^*GFEFCC + 18^*GBBETA + 5000$
no ternary parameters
T – THERNARY PHASE
3 sublattices, sites 0.32:0.28:0.4
constituents: V:Fe:B
$^T G_{V:FE:B;0} - 0.4^*H298(BETA\_rhombo\_b,B;0) - 0.28^*H298(BCC\_A2,FE;0)$
$- 0.32^*H298(BCC\_A2,V;0) = -49,198.19 + 3.73^*T + 0.32^*GVBCC + 0.28^*GFEBCC$
$+ 0.4^*GBBETA$
V₂B₃
2 sublattices, sites 0.4:0.6
constituents: Fe,V:B
$^{V_2B_3}G_{Fe:B;0} - 0.6^*H298(BETA\_rhombo\_b, B; 0) - 0.4^*H298(BCC\_A2, FE; 0) =$
$+0.4^*GFEBCC + 0.6^*GBBETA + 5000$
$^{V_2B_3}L_{Fe,V:B;0} = -44,970 + 6.3^*T$ 298.00 < T < 4000.00
V₃B₂
2 sublattices, sites 0.6:0.4
constituents: Fe,V:B
$^{V_3B_2}G_{Fe:B;0} - 0.4^*H298(BETA\_rhombo\_b, B; 0) - 0.6^*H298(BCC\_A2, FE; 0) =$
$+0.6^*GFEBCC + 0.4^*GBBETA + 5000$
$^{V_3B_2}L_{Fe,V:B;0} = -61,338.0467 + 10.3015864^*T$ 298.00 < T < 4000.00
V₃B₄
2 sublattices, sites 0.4286:0.5714
constituents: Fe,V:B
$^{V_3B_4}G_{Fe:B;0} - 0.5714^*H298(BETA\_rhombo\_b, B; 0) -$
$0.4286^*H298(BCC\_A2, FE; 0) = +0.4286^*GFEBCC + 0.5714^*GBBETA + 5000$
$^{V_3B_4}L_{Fe,V:B;0} = -103,265.443 + 27.61444^*T$ 298.00 < T < 4000.00
$^{V_3B_4}L_{Fe,V:B;1} = -73,669.492 + 10.364^*T$ 298.00 < T < 4000.00
$^{V_3B_4}L_{Fe,V:B;2} = -13,946.67 - 17.7^*T$ 298.00 < T < 4000.00
V₅B₆
2 sublattices, sites 0.4545:0.5455
constituents: Fe,V:B
$^{V_5B_6}G_{Fe:B;0} - 0.5455^*H298(BETA\_rhombo\_b, B; 0) -$
$0.4545^*H298(BCC\_A2, FE; 0) = +0.4545^*GFEBCC + 0.5455^*GBBETA + 5000$
$^{V_5B_6}G_{V:B;0} - 0.5455^*H298(BETA\_rhombo\_b, B; 0) -$
$0.4545^*H298(BCC\_A2, V; 0) =$
$+0.4545^*GVBCC + 0.5455^*GBBETA - 67,868.58 + 6.3429^*T$
$^{V_5B_6}L_{Fe,V:B;0} = -42,965 + 3.85^*T$ 298.00 < T < 4000.00
VB
2 sublattices, sites 0.5:0.5
constituents: Fe,V:B
$^{VB}G_{Fe:B;0} - 0.5^*H298(BETA\_rhombo\_b,B;0) - 0.5^*H298(BCC\_A2,FE;0)$
$= +0.5^*GFEBCC + 0.5^*GBBETA + 5000$

Table 3 (*Continued*)

$^{VB}L_{Fe,V:B;0} = -27,718.9286 - 6.78571428^*T$ 298.00 < T < 4000.00
VB₂
2 sublattices, sites 0.333:0.667
constituents: Fe,V:B
$^{VB_2}G_{Fe:B;0} - 0.667^*H298(BETA\_rhombo\_b, B; 0) - 0.333^*H298(BCC\_A2, FE; 0) =$
$+0.333^*GFEBCC + 0.667^*GBBETA + 5000$
$^{VB_2}L_{Fe,V:B;0} = -105,146.429 + 60.7142857^*T$ 298.00 < T < 4000.00
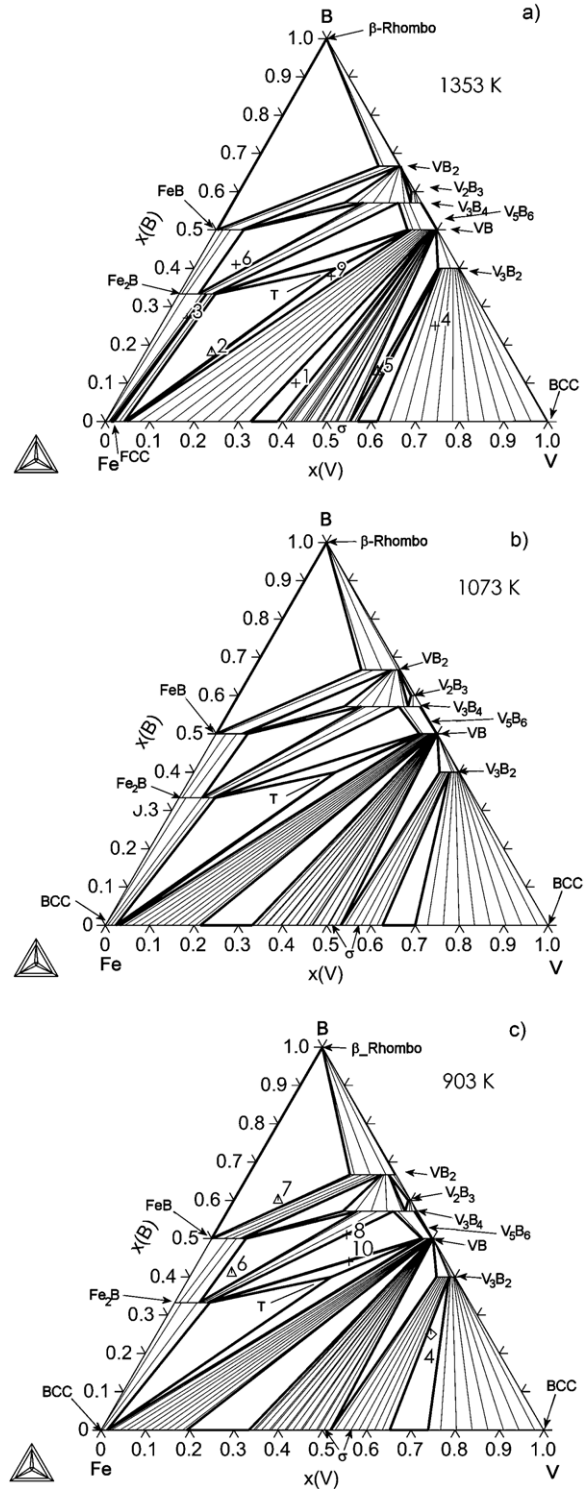
Fig. 5. Calculated isothermal section of the phase diagram of Fe–B–V system, at (a) 1353 K with marked experimental alloys (+, three phase field; △, two phase field), (b) 1073 K, (c) 903 K with marked experimental alloys (+, three phase field; △, two phase field; ◇, nonequilibrium structure).
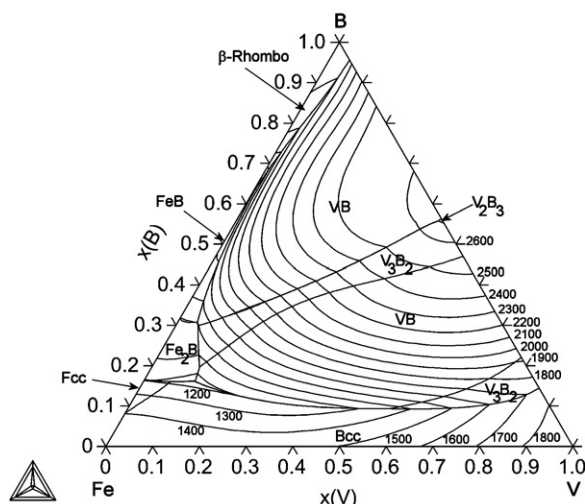
Fig. 6. Liquidus surface prediction calculated with using new database for Fe–B–V system.

with our experimental results and that at 1073 K was compared with phase analysis available in the work of Kuzma and Starodub [2].

Results of phase analyses for alloys 3, 4, 5, and 6 at 1353 K are in very good agreement with calculations, Fig. 5a. The alloys 1, 2, and 9 does not completely correspond to the calculated equilibria, nevertheless, they exhibit the phase composition corresponding to the neighbouring phase field. With respect to certain uncertainities in the establishing of the precise overall composition of alloys, this agreement is very good.

Main difference between our calculated phase diagram at 1073 K and experimental results by Kuzma and Starodub [2] is the existence of the ternary phase. Kuzma and Starodub did not found any new phase in their study. It is not possible to identify why, as no detailed information about alloys and experimental measurement setup are mentioned in their paper.

However, small differences close to the Fe–V binary diagram exist. The two-phase field (σ + BCC) is shifted more towards the centre of the diagram on both sides of the Fe–V binary diagram, and corresponding σ one-phase field is narrower in the paper [2] in comparison with our calculations, Fig. 1a. This discrepancy can be explained by different Fe–V binary diagram used in the paper [2]. The Fe–V binary data assessment made by Huang [9] and used in our calculations is generally accepted for the modelling in recent literature, for example [12–14].

High solubility of iron in V_3B_4 boride is in agreement with paper [2]. Similarly, the solubility of third element in the other borides is comparable with that given in [2].

The comparison of our experimental results and calculations for 903 K showed that results for alloys 6, 7, 8, and 10 are in good agreement with calculations, Fig. 5c. In the alloy 4, VB boride was identified after annealing. Its existence cannot be expected in this alloy in equilibrium. The reason for the VB boride presence in the alloy can be explained by its formation during cooling after the alloy production in argon arc furnace. This is supported by the V–B binary diagram, Fig. 1b, where the VB boride solidifies as a primary phase for the alloy with approx. 25 at.% of B between approx. 2500–2200 K. Because of low temperature of annealing and consequent slow dissolution rate, used time of annealing (190 days) seems not to be sufficient for its dissolution.

The comparison of theoretical modelling and results of experimental measurements shows that developed database describes phase equilibria in the system quite well.

5.2. Ternary phase T

Ternary phase T was found in alloy 2 at 1353 K. Its boron content is approx. 40 at.%, it also contains approx. 28 at.% of Fe. The B content is similar to the V_3B_2 boride; nevertheless the existence of V_3B_2 boride with very high solubility of iron in this region of the phase diagram is not possible because of other experimental results. No V_3B_2 boride was found in alloys 1, 5, 9 (see Fig. 2a). Mentioned alloys should contain this boride if the T phase were V_3B_2 boride with high content of Fe. Also, alloy 2 was studied by X-ray diffraction and T phase was not identified as a phase based on any known binary boride. Therefore we suppose that T phase is a ternary phase with very narrow homogeneity range as shown in the phase diagram, Fig. 5. Also, the amounts of existing phases in alloy 2 correspond to the nominal composition of this alloy. There is very small amount of vanadium boride VB that is mainly embedded in the particles of T phase, Fig. 2a. The amounts of T and BCC phases in alloy 2 are approximately the same.

Further experimental measurements and calculations are needed for the determination of complete crystallographic information of T phase.

The database was also used to calculate liquidus surface prediction of the system, Fig. 6. However no experimental results about liquidus of the ternary system are known which does not allow its experimental verification at this moment.

6. Conclusions

The work deals with modelling of Fe–B–V phase diagram by CAL-PHAD method using our experimental measurements and available experimental literature data. The achieved results can be summarised as follows:

- Boron is modelled as interstitial element in solid solutions (BCC, FCC); all borides are modelled as stoichiometric phases with respect to boron. New ternary phase T is modelled as stoichiometric phase.
- New ternary phase T (with chemical composition 28Fe32V40B in at.%) was found in 67Fe–18B–15V [in at.%] alloy at 1353 K. Further experimental measurements for crystallographic information determination of ternary phase are needed.
- Good agreement between experimental results and calculations was found.

References

[1] H. Ohtani, M. Hasebe, K. Ishida, T. Nishizawa, Trans. ISIJ 28 (1988) 1043–1050.
[2] J.B. Kuzma, P.K. Starodub, Neorganiceskije Materialy 3 (1973) 376–381.
[3] M. Hillert, L.I. Staffansson, Acta Chem. Scand. 24 (1970) 3618–3626.
[4] T. Van Rompacy, K.C. Hari Kumar, P. Wollants, J. Alloys Compd. 334 (2002) 173–181.
[5] K. Tanaka, T. Saito, J. Phase Equilib. 20 (1999) 207–214.
[6] B. Hallemans, P. Wollants, J.R. Roos, J. Phase Equilib. 16 (1995) 137–149.
[7] C. Guo, P.M. Kelly, Mater. Sci. Eng. A352 (2003) 40–45.
[8] http://www.thermocalc.se.
[9] W. Huang, Z. Metallkd. 82 (1991) 391–395.
[10] A.T. Dinsdale, Calphad 15 (1991) 317–425.
[11] SSOL Database, The SGTE DATABASE for Solutions, 1993, http://www.thermocalc.se/res/pdfDBD/DBD_SSOL4-2.pdf.
[12] E. Fras, M. Kavalec, H.F. Loper, Mater. Sci. Eng. A524 (2009) 193–203.
[13] C.P. Wang, X.J. Liu, I. Ohnuma, R. Kainuma, K. Ishida, J. Phase Equilib. 23 (2002) 236–245.
[14] SGSOL alloy solution database, 2010, http://resource.npl.co.uk/mtdata/mtdata software.htm.